

A molecular-beam optical Stark study of lines in the (1,0) band of the $F^4\Delta_{7/2}-X^4\Delta_{7/2}$ transition of iron monohydride, FeH

Timothy C. Steimle^{a)} and Jinhai Chen

Department of Chemistry and Biochemistry, Arizona State University, Tempe, Arizona 85287-1604

Jeremy J. Harrison and John M. Brown

Physical and Theoretical Chemistry Laboratory, University of Oxford, South Parks Road, Oxford, OX1 3QZ, United Kingdom

(Received 2 March 2006; accepted 17 March 2006; published online 8 May 2006)

A supersonic molecular beam of iron monohydride, FeH, has been generated using a laser ablation/chemical reaction scheme and probed at near-natural linewidth resolution by optical Stark spectroscopy utilizing laser-induced fluorescence detection. The observed Stark splitting in $Q(3.5)$ and $R(3.5)$ lines of the $F^4\Delta_{7/2} \leftarrow X^4\Delta_{7/2}$ (1,0) transition were analyzed to determine values for the magnitudes of the permanent electric dipole moments, $|\mu|$, which were found to be 2.63(3) and 1.29(3) D for the $X^4\Delta$ ($v=0$) and $F^4\Delta$ ($v=1$) states, respectively. A comparison with *ab initio* theoretical predictions is made. The Λ doubling in the low- J levels of the $F^4\Delta_{7/2}$ ($v=1$) state is also modeled. © 2006 American Institute of Physics. [DOI: 10.1063/1.2194551]

I. INTRODUCTION

Iron monohydride, FeH, is the most thoroughly studied transition-metal monohydride. Some time ago intense near-infrared emission spectral features of this molecule were recorded using Fourier transform (FT) spectroscopy.¹ A band near 1 μm was assigned to the $F^4\Delta \rightarrow X^4\Delta$ electronic transition and rotationally analyzed. This band, known as the Wing-Ford band, has been the subject of further analysis and modeling² because of its prevalence in the emission of the M -type and cooler stars. Recently, additional near-infrared emission bands at 1.58 and 1.35 μm that appeared in the original FT recording¹ were assigned to the $E^4\Pi \rightarrow A^4\Pi$ and $E^4\Pi \rightarrow X^4\Delta$ electronic transitions, respectively, and rotationally analyzed.³ Alongside the analysis of the FT-recorded near-infrared emission spectrum, a series of laser-induced fluorescence (LIF) and dispersed-fluorescence (DF) measurements of numerous visible band systems^{4–12} have been made. These have identified the low-lying $a^6\Delta$ (Refs. 5, 6, 8, 10, and 11), $C^4\Phi$,⁹ $b^6\Pi$,^{9,11} and $c^6\Sigma^+$ (Refs. 7 and 8) states, all below 10 000 cm^{-1} . The most detailed information for the $X^4\Delta$ state comes from the far-infrared (FIR), pure rotational,¹³ and midinfrared (MIR), vibrational,¹⁴ laser magnetic resonance (LMR) spectroscopic studies. Analysis of the FIR-LMR spectra has recently been completed¹⁵ and is essential to the analysis performed here. A review of the spectroscopy can be found in Refs. 2, 3, and 15.

Modeling the fine-structure energy-level patterns within the low-lying electronic states of FeH,^{1–12} as well as the magnetic tuning of transitions in the $X^4\Delta$ state,^{13–15} has proven to be exceedingly difficult. None of the numerous recorded band systems have been adequately fit using an effective Hamiltonian. In such an approach, the effects of rotational- and spin-orbit-induced mixings of the various

Born-Oppenheimer vibronic states are projected onto the state of interest by the use of perturbation theory. The detection of so many low-lying electronic states suggests a severe breakdown of the Born-Oppenheimer approximation: the assumption that each total wave function is restricted to a single electronic surface. The numerous Born-Oppenheimer limited, electronic-structure calculations for FeH (Refs. 16–21) reveal that the root cause of this breakdown is the importance of both the $3d^64s^2$ and $3d^74s^1$ configurations in the bonding description of the numerous low-lying states.

It is helpful to think of the bonding within FeH as arising from the interaction of neutral iron with hydrogen. Most calculations predict that as an Fe atom in its ground state (a^5D , arising from the $3d^64s^2$ configuration) approaches a ground-state H atom, the d electrons remain high-spin coupled, whereas the s electrons become hybridized due to a mixing with the $3d^64s^14p^1$ configuration. This mixing is efficient because the lowest-lying term of this configuration, z^7D , is only 19 350 cm^{-1} above the ground term. Bonding occurs by the interaction of the $4s/4p$ hybrid orbital with the H $1s$ orbital, the resultant bonding orbital being doubly occupied. The associated nonbonding $4s/4p$ σ -type hybrid orbital, which points away from the Fe–H bond, is singly occupied. The electron in this σ -type hybrid orbital couples with the high-spin-coupled $3d^6$ electrons, resulting in six possible states: $^4\Delta$, $^4\Phi$, and $^4\Sigma^+$. If an Fe atom in its low-lying a^5F state, arising from the $3d^74s^1$ configuration, approaches a ground-state H atom, the bonding is more straightforward. A simple $\text{Fe}(4s)+\text{H}(1s)$ bonding orbital is formed and has double occupation. The $3d^7$ electrons remain high-spin coupled, and only four quartet states are allowed: $^4\Phi$, $^4\Delta$, $^4\Pi$, and $^4\Sigma^-$ states. Since $^4\Delta$ and $^4\Pi$ terms can arise from both the $3d^64s^2$ and $3d^74s^1$ configurations of Fe, the low-lying $^4\Delta$ and $^4\Pi$ states of FeH are highly stabilized (configuration interaction).¹⁸ In total there are ten electronic states, with 46 associated spin-orbit components, all lying below

^{a)}Electronic mail: Tsteimle@ASU.edu

10 000 cm^{-1} ; of these the $F^4\Delta$ and $X^4\Delta$ states are, according to this simple picture, strong admixtures of the $3d^74s^1$ and $3d^64s^2$ configurations. There is strong spin-orbit and rotational mixing between the two groups of states because their configurations differ by only one spin orbital. Given that the $v=1$ levels for the $X^4\Delta$ and $F^4\Delta$ states lie 1759 and 1422 cm^{-1} ,¹ respectively, above the $v=0$ ones, and that the spin-orbit interaction and rotational mixing are both large, then the Born-Oppenheimer approximation is not valid and the effective Hamiltonian approach inappropriate. Furthermore, due to the neglect of the nonadiabatic and spin-orbit mixing terms in reported *ab initio* calculations, it is unlikely that the current quantum-mechanical calculations will quantitatively predict experimental observations.

The dipole moment is very sensitive to the balance between the two types of bonding mechanism and hence is an important diagnostic of the quality of predicted wave functions. The $\text{Fe}(3d^74s^1)+\text{H}(1s^1)$ bonding mechanism leads to a $(4s+1s)$ bond polarized towards the H center and hence a large dipole moment. The $\text{Fe}(3d^64s^2)+\text{H}(1s^1)$ bonding mechanism which involves $4s/4p$ hybridization leads to an unpaired electron in an orbital that points away from the H center and hence a small dipole moment. The prediction by Chong *et al.*¹⁶ for the $X^4\Delta$ state using complete-active space self-consistent field (CASSCF) followed by various forms of multireference configuration interaction (MRCI) treatment of dynamical electron correlation exhibited wide variation ranging from 4.300 D when the MRCI is single and double excitation (SDCI) to 1.334 D when a coupled pair functional approach (CPF) is used. A value of 2.9 ± 0.2 D was obtained for $\mu(X^4\Delta)$ from extrapolation of a natural orbital (NO) iteration performed to optimize the orbitals from the CASSCF/CI prediction. The slow convergence of the NO iteration from the CASSCF/CI value of 1.73 D to the estimated value of 2.9 ± 0.2 D shows that it is difficult to remove the bias towards the $3d^64s^2$ configuration, which results in $4s/4p$ hybridization and smaller values for $\mu(X^4\Delta)$. The use of an energy-adjusted *ab initio* pseudopotential to represent the Ne-like core predicts 3.77 D for $\mu(X^4\Delta)$.¹⁷ A CASSCF calculation combined with a multireference coupled pair approximation [MRCPA(4)] for treatment of dynamical electron correlation predicts 2.59 and 2.43 D for $\mu(X^4\Delta)$ and $\mu(F^4\Delta)$, respectively.²⁰ These results suggest that the $3d^64s^2$ and $3d^74s^1$ configurations are of comparable importance in describing the two states. Recently, Wang *et al.*²¹ predicted 2.1 and 0.2 D for $\mu(X^4\Delta)$ and $\mu(F^4\Delta)$, respectively, using a very similar CASSCF approach for generating the configuration state functions but then employing a multireference SDCI approach. These results suggest that the $3d^64s^2$ configuration is more important in the description of the $F^4\Delta$ state than it is in the $X^4\Delta$ state.

II. EXPERIMENT

Iron monohydride was generated by laser ablation of a solid iron metal sample in a pure hydrogen, pulsed, supersonic expansion. Typically the conditions were 2000 kPa backing pressure, and 5 mJ of loosely focused ($f=0.5$ m), 355 nm radiation from a frequency tripled Nd: yttrium alu-

minum garnet (YAG) laser. The supersonic free-jet expansion was skimmed to produce a well collimated molecular beam. The differentially pumped molecular-beam chamber and optical Stark spectrometer has been described previously.²² Approximately 100 mW of lightly focused ($f=1.0$ m) power derived from a single longitudinal mode cw-Ti: sapphire laser was used to excite lines in the $F^4\Delta_{7/2}\leftarrow X^4\Delta_{7/2}$ (1,0) band near 880 nm. The resulting laser-induced fluorescence was viewed through an 880 ± 10 nm band pass filter and detected with a cooled GaAs photo-multiplier tube. Photon-counting techniques were used to process the signal. The $F^4\Delta_{7/2}\leftarrow X^4\Delta_{7/2}$ (1,0) band was selected for study because the (0,0) band near 1000 nm lies too far in the infrared for detection with the GaAs photomultiplier tube. The Franck-Condon factor for the (1,0) band ($=0.1349$) is much less than that for the (0,0) band ($=0.8338$).² Wavelength calibration was obtained by simultaneously recording of the absorption spectrum of a heated I_2 cell.^{23,24} The number of precisely measured I_2 features is relatively sparse in portions of the desired spectral range and long extrapolations were performed by monitoring the transmission of an actively stabilized, 753.58 MHz free spectral range (f.s.r.), confocal étalon²⁵ along with the LIF signal.

Static electric fields approaching 5000 V/cm were created by application of a voltage across a pair of conducting, 95% transmitting, neutral density filter plates in a parallel arrangement and spaced about 2.54 cm apart. A polarization rotator and polarizing filter were used to set the electric-field vector of the linearly polarized laser radiation either parallel or perpendicular to the static electric field resulting in $\Delta M_F=0$ or $\Delta M_F=\pm1$ selection rules. The relative transition frequencies of the electric-field-induced Stark shifts, and splittings were determined by simultaneously recording the transmission of the excitation laser through the actively stabilized 753.58 MHz f.s.r. to establish a wavelength scale for various scans and an unstabilized 75.4 MHz f.s.r. confocal étalon for extrapolations within a given scan. The systematic error introduced by spectral calibration procedures and electric-field strength determination is estimated to be approximately 2%.

III. OBSERVATIONS

This is the first molecular-beam study of the FeH radical. The low-rotational features with $J''<7.5$ of the (1,0) band of the $F^4\Delta_{7/2}\leftarrow X^4\Delta_{7/2}$ transition were recorded field-free and the determined transition wave numbers are presented in Table I. The values agree with those obtained from the Doppler-limited spectra to within the ±0.02 cm^{-1} uncertainty of that work. The accuracy of the present measurements is estimated to be the ±0.003 cm^{-1} of the I_2 calibration.^{22,23} The observed and predicted spectra for the $Q(3.5)$ and $R(3.5)$ lines are presented in Fig. 1. The partially resolved structure, which was not resolved in the thermal emission spectra,¹ is due to Λ doubling and the proton magnetic hyperfine interaction. The Λ doubling increases rapidly with increasing rotation in both the $F^4\Delta_{7/2}$ and $X^4\Delta_{7/2}$ states and each of the P -, Q -, and R -branch features with $J''>3.5$ appear as doubled. The Λ doubling in the $X^4\Delta_{7/2}$ state is about five times greater than that in the $F^4\Delta_{7/2}$ state. The observed and

TABLE I. Zero-field measurements of lines in the (1,0) band of the $F^4\Delta_{7/2} \leftarrow X^4\Delta_{7/2}$ transition of FeH.

Line	Parity	F	Wave number (cm ⁻¹)
$P(4.5)$	$+\leftarrow-$	$4\leftarrow 5$	11 309.6470 ^a
	$+\leftarrow-$	$3\leftarrow 4$	11 309.6483
	$-\leftarrow+$	$4\leftarrow 5$	11 309.6578
	$-\leftarrow+$	$3\leftarrow 4$	11 309.6593
$Q(3.5)$	$-\leftarrow+$	$4\leftarrow 4$	11 356.7254
	$-\leftarrow+$	$3\leftarrow 3$	11 356.7269 ^b
	$+\leftarrow-$	$4\leftarrow 4$	11 356.7269 ^b
	$+\leftarrow-$	$3\leftarrow 3$	11 356.7284
$Q(4.5)$	$+\leftarrow-$	^c	11 358.1831
	$-\leftarrow+$	^c	11 358.1928
$Q(5.5)$	$-\leftarrow+$	^c	11 359.1912
	$+\leftarrow-$	^c	11 359.2275
$R(3.5)$	$-\leftarrow+$	$5\leftarrow 4$	11 405.2601
	$-\leftarrow+$	$4\leftarrow 3$	11 405.2618 ^b
	$+\leftarrow-$	$5\leftarrow 4$	11 405.2618 ^b
	$+\leftarrow-$	$4\leftarrow 3$	11 405.2635
$R(4.5)$	$+\leftarrow-$	^c	11 417.4509
	$-\leftarrow+$	^c	11 417.4635
$R(5.5)$	$-\leftarrow+$	^c	11 429.1578
	$+\leftarrow-$	^c	11 429.2040
$R(6.5)$	$+\leftarrow-$	^c	11 440.0569
	$-\leftarrow+$	^c	11 440.2702
$R(7.5)$	$-\leftarrow+$	^c	11 449.8529
	$+\leftarrow-$	^c	11 450.1136

^aAccuracy of a single measurement = 0.003 cm⁻¹; relative measurements reliable to 0.0003 cm⁻¹.

^bBlended lines.

^cProton hyperfine splitting not resolved.

calculated $P(4.5)$ lines and associated energy level pattern are presented in Fig. 2. The 315 MHz splitting in the spectrum is due to the Λ doubling in the $J=4.5$ $X^4\Delta_{7/2}$ ($v=0$) level. The small splitting in the two $P(4.5)$ lines is due to proton magnetic hyperfine interaction in the $J=4.5$ Λ doublets of the $X^4\Delta_{7/2}$ state. These splittings have been determined to be 48 and 41 MHz for the upper and lower energy Λ -doublet components, respectively.¹⁵ The hyperfine splitting in the $F^4\Delta_{7/2}$ state is negligible.

The $Q(3.5)$ and $R(3.5)$ lines of the $F^4\Delta_{7/2} \leftarrow X^4\Delta_{7/2}$ (1,0) band were selected for the Stark measurements because they are associated with the nearly degenerate Λ doublet (splitting ≈ 50 MHz) of the $J=3.5$ rotational level of the $X^4\Delta_{7/2}$ ($v=0$) state. The $J=3.5$ and $J=4.5$ $F^4\Delta_{7/2}$ ($v=1$) levels, which are the upper termini of these two spectral features, have Λ -doubling intervals of approximately 0 and 20 MHz, respectively. Therefore, the energy levels associated with the $Q(3.5)$ and $R(3.5)$ lines will exhibit a strong, nearly linear, Stark tuning. The $Q(3.5)$ line recorded field free and in the presence of a static electric field at 667 V/cm of parallel polarization and 627 V/cm of perpendicular polarization are presented in Figs. 3 and 4, respectively. The associated energy levels as functions of applied electric field and the spectral assignments are given on the right-hand side of these figures. The nuclear spin decouples rapidly from the molecular axis in the $J=3.5$ level of the $X^4\Delta_{7/2}$ ($v=0$) state upon application of the electric field because of the smallness

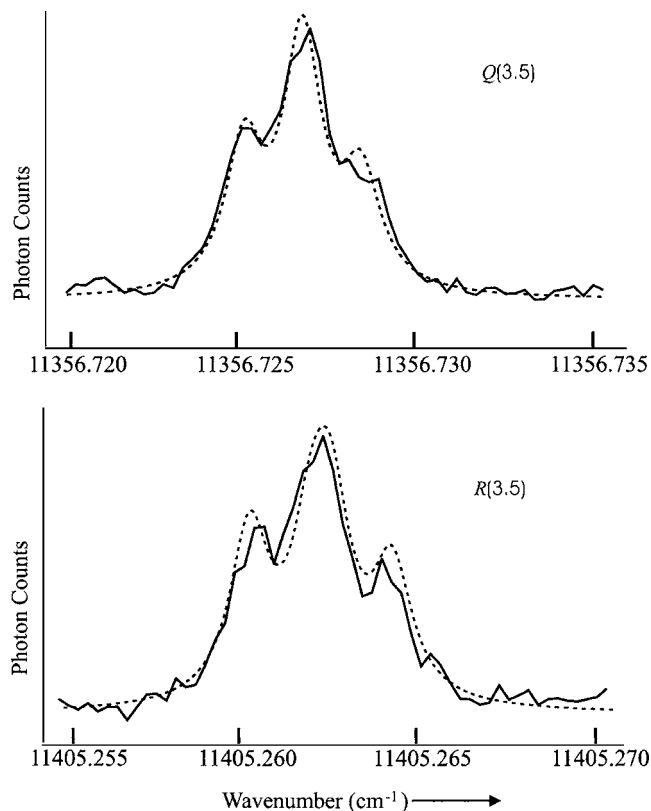


FIG. 1. The observed (solid line) and predicted (dashed line) $Q(3.5)$ and $R(3.5)$ lines in the $F^4\Delta_{7/2} \leftarrow X^4\Delta_{7/2}$ (1,0) band of FeH. The unresolved structure is due to Λ doubling and proton magnetic hyperfine splitting in the $X^4\Delta_{7/2}$ ($v=0$) state.

of the proton hyperfine interaction. The approximately good quantum numbers become M_J ($=-3.5$ to $+3.5$) and M_I ($=\pm 0.5$) and the energy level pattern consists of eight ($=2J+1$) sets of proton hyperfine-split doublets. The spectroscopic selection rules become $\Delta M_J = \pm 1$ and $\Delta M_J = 0$ for perpendicular and parallel polarizations, respectively, with the

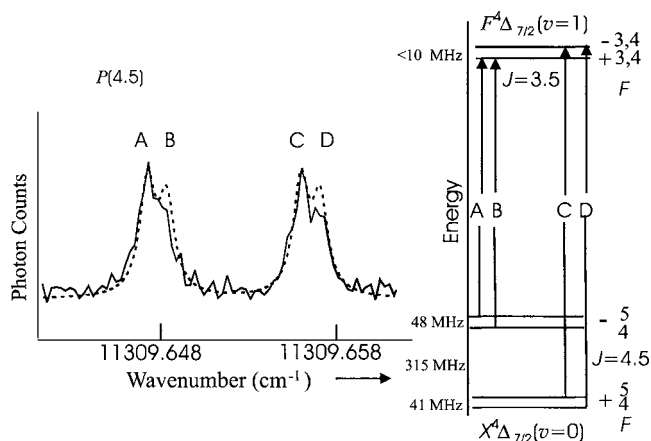


FIG. 2. The observed (solid line) and predicted (dashed line) structure of the $P(3.5)$ line in the $F^4\Delta_{7/2} \leftarrow X^4\Delta_{7/2}$ (1,0) band of FeH and associated energy levels. The Λ doubling in the $J=4.5$ $X^4\Delta_{7/2}$ ($v=0$) level is 315 MHz and for the $J=3.5$ $F^4\Delta_{7/2}$ ($v=1$) level approximately 0 MHz. The unresolved structure is due to Λ doubling and proton magnetic hyperfine splitting in the $X^4\Delta_{7/2}$ ($v=0$) state. The proton magnetic hyperfine splittings for the Λ doublets of the $J=4.5$ $X^4\Delta_{7/2}$ ($v=0$) levels are approximately 44 MHz and approximately 0 MHz for the Λ doublets of the $J=3.5$ $F^4\Delta_{7/2}$ ($v=1$) levels.

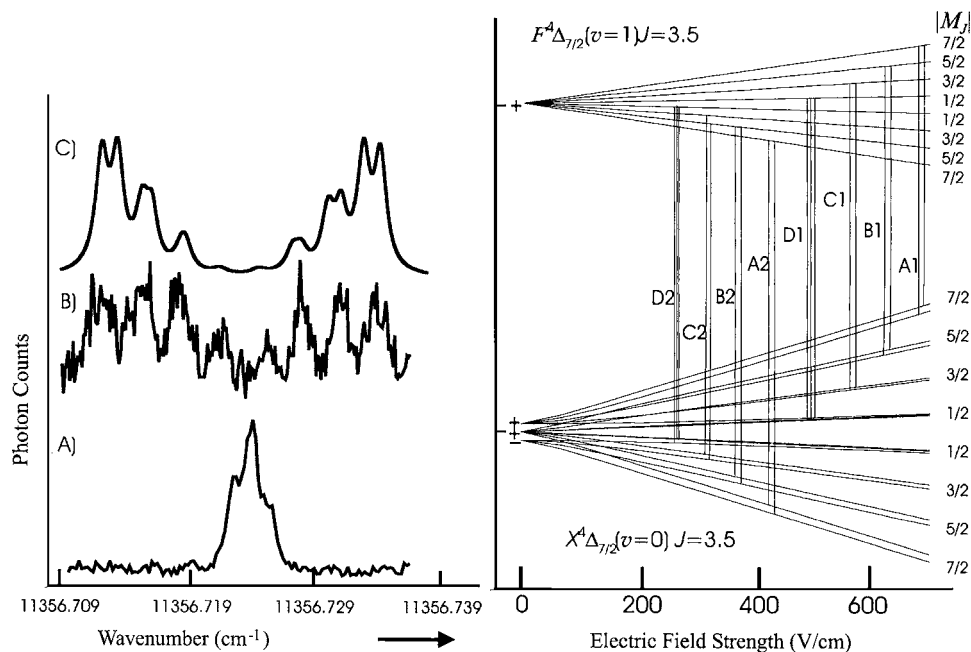


FIG. 3. The $Q(3.5)$ line observed field-free (A); in the presence of an electric-field strength of 667 V/cm polarized parallel ($\Delta M_J=0$) to the laser field (B); and the predicted spectrum (C). The predicted energy levels as a function of field strength and the spectral assignments are given in the right side of the panel.

additional requirement that $\Delta M_J=0$. The eight strong $\Delta M_J=0$ spectral features of the $Q(3.5)$ parallel Stark spectra are resolved in Fig. 3 and are labeled as “A₁-D₁” and “A₂-D₂.” Only ten of the fourteen $\Delta M_J=\pm 1$ transitions are resolved and are labeled by “A” through “J” in Fig. 4. The central four features are an overlap of both $\Delta M_J=\pm 1$ transitions as indicated in the energy level pattern of this figure. Most of features in Figs. 3 and 4 correlate with parity-allowed transitions in the absence of applied field, the noticeable exception being contributions to the “D” and “G” components of the perpendicular transition.

The $R(3.5)$ line observed in the presence of an electric-field strength of 667 V/cm polarized parallel to the laser field ($\Delta M_J=0$) along with the predicted Stark spectrum, associated energy levels and assignment are presented in Fig. 5. All eight strong $\Delta M_J=0$ spectral features are resolved and are labeled “A-H.” The $R(3.5)$ line observed in the presence of a perpendicular field was too severely overlapped to make an assignment.

The data set consists of 126 distinct Stark features, which have been assigned to a total of 364 Stark shifts, associated with the $Q(3.5)$ parallel, $Q(3.5)$ perpendicular, and $R(3.5)$ parallel spectra recorded at numerous field strengths ranging from 510 to 745 V/cm. The measured shifts, assignments, and the differences between the observed and calculated shifts for the three spectral features are available via the Electronic Physics Auxiliary Publication Service (EPAPS) or through one of the authors (T.C.S.).²⁶

IV. ANALYSIS

A. Field free

Modeling the field-free Λ doubling and hyperfine splittings within a given rotational level of the $X^4\Delta_{7/2}(v=0)$ and $F^4\Delta_{7/2}(v=1)$ levels of FeH is a prerequisite to modeling the Stark effect. The Λ doubling and hyperfine splittings in the $X^4\Delta_{7/2}(v=0)$ level have been accurately determined over the $J=3.5$ to 7.5 range.¹⁵ The splittings are resolved in the

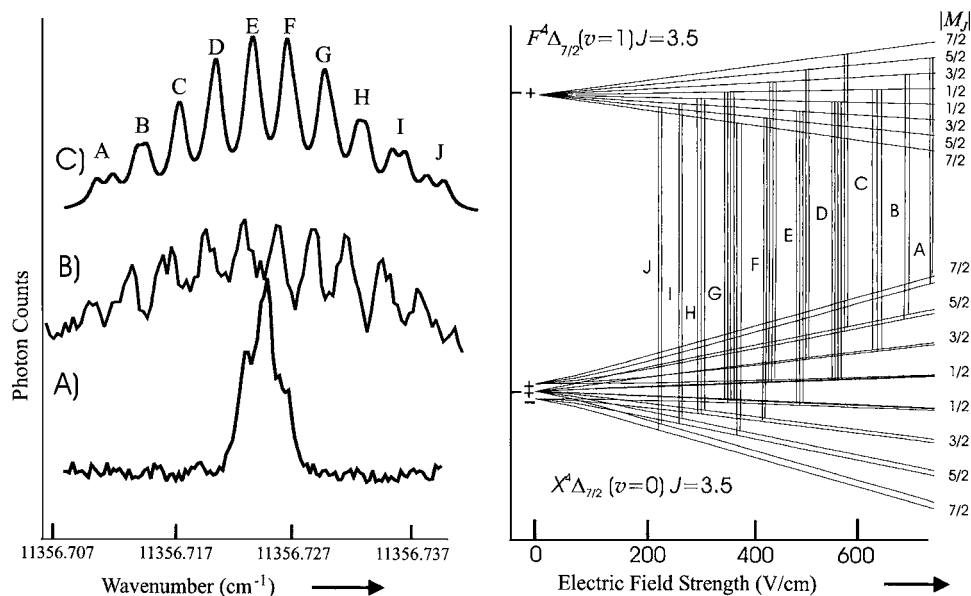


FIG. 4. The $Q(3.5)$ line observed field free (A); in the presence of an electric-field strength of 627 V/cm polarized perpendicular ($\Delta M_J=\pm 1$) to the laser field (B); and the predicted spectrum (C). The predicted energy levels as a function of field strength and the spectral assignments are given in the right side of the panel.

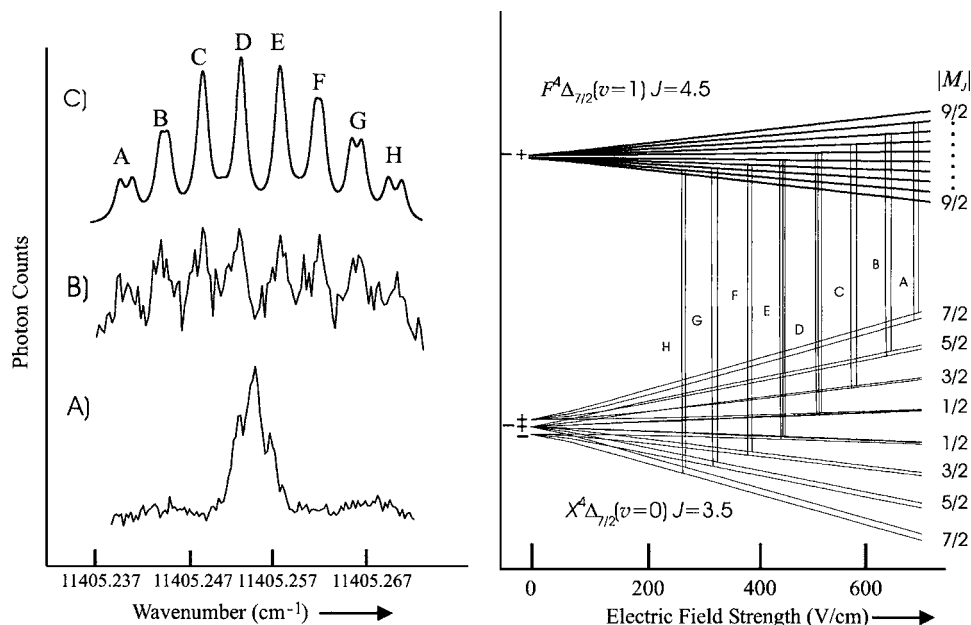


FIG. 5. The $R(3.5)$ line observed field free (A); in the presence of an electric-field strength of 667 V/cm polarized parallel ($\Delta M_J=0$) to the laser field (B); and the predicted spectrum (C). The predicted energy levels as a function of field strength and the spectral assignments are given in the right side of the panel. The Λ doubling in the $J=4.5$ $F^4\Delta_{7/2}$ ($v=1$) level is approximately 20 MHz.

present work and their inclusion is essential to the analysis. However, the Λ doubling and hyperfine splittings over a range of J values in both the $X^4\Delta_{7/2}$ ($v=0$) and $F^4\Delta_{7/2}$ ($v=1$) states exhibit some irregularities and cannot be modeled using an effective Hamiltonian operator. Despite this, the effective Hamiltonian can still be used over a small range of J values to obtain reliable energies and eigenvectors. Any molecular parameters so obtained are only meaningful over the small range of rotational levels to which they apply.

Although accurate term values have been determined experimentally for the low- J levels of the $X^4\Delta_{7/2}$ ($v=0$) state,¹⁵ the corresponding levels of the $F^4\Delta_{7/2}$ ($v=1$) state are not known to such high precision. The present measurements, when combined with the ground-state splittings,¹⁵ show that the hyperfine effects in the low- J features ($J<8.5$) of the $F^4\Delta_{7/2}$ ($v=1$) state were not detectable. The Λ doubling for the $J=3.5, 4.5, 5.5, 6.5, 7.5$, and 8.5 levels were determined to be 0, 20, 59, 190, 2845, and 732 MHz, respectively, and are plotted in Fig. 6. These splittings, with the exception of

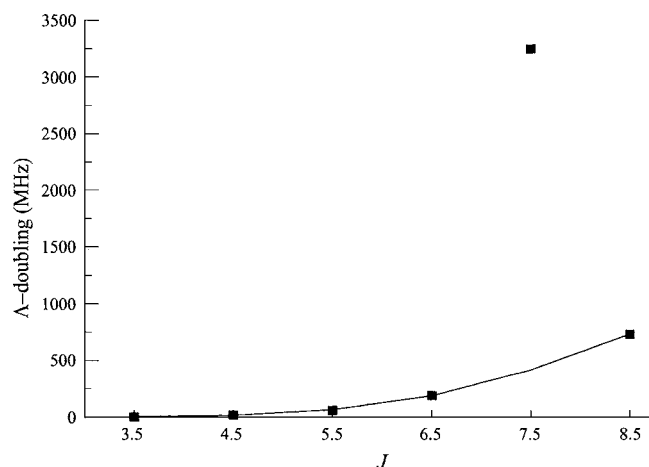


FIG. 6. The observed Λ doubling in the low- J levels of FeH in the $F^4\Delta_{7/2}$ ($v=1$) state. The solid line is a result of a prediction using the optimized parameters of Eq. (1) when all but the $J=7.5$ data point are included.

the 2845 MHz value for $J=7.5$, were modeled by a third-order perturbation treatment of the Λ -doubling effects within $a^4\Delta_{7/2}$ spin component,²⁷

$$\Delta E_{LD} = [\delta + \delta_D J(J+1)](J^2 - 0.25)(J^2 - 2.25)(J^2 - 6.25) \times (J+3.5), \quad (1)$$

where δ is an effective Λ -doubling parameter, and δ_D its centrifugal distortion correction. The $J=3.5, 4.5, 5.5, 6.5$, and 8.5 splittings were least-squares fit to Eq. (1) to obtain values for δ and δ_D of $1.534(50) \times 10^{-8}$ and $-1.027(63) \times 10^{-10} \text{ cm}^{-1}$, respectively.

It was necessary to obtain approximate eigenvectors in addition to eigenvalues to model the spectral intensities, upon which the correct assignments of the Stark-shifted components depend. The angular momentum coupling in the lowest J levels of both the $X^4\Delta_{7/2}$ ($v=0$) and $F^4\Delta_{7/2}$ ($v=1$) states conforms closely to that of a molecule in a Hund's case ($a_{\beta J}$) limit with the spin-orbit splitting larger than the rotational spacing which in turn is much larger than the hyperfine splitting. The field-free eigenvalues and eigenvectors were obtained by numerical diagonalization of a 4×4 matrix representation constructed using a Hund's case ($a_{\beta J}$) nonparity basis set; $\Psi = |n\Lambda; S\Sigma; J\Omega IFM_F\rangle$ with $\Sigma = \pm 3/2$, $\Lambda = \pm 2$, and $\Omega = \pm 7/2$. Explicit experimental energies were used to reproduce the rotational and Λ -doubling effects. Specifically for the $v=0$ level of the $X^4\Delta_{7/2}$ state, the average term energies of the two Λ doublets given in Ref. 15 were used for the diagonal elements in the representation of the rotational operator, H^{rot} . The Λ doubling was modeled by halving the experimental doublings in Ref. 15 for the $\langle \Lambda \pm 2, J | H^{\text{LD}} | \Lambda \mp 2, J \rangle$ off-diagonal elements in the representation of the Λ -doubling operator, H^{LD} .

Reproducing the proton magnetic hyperfine interaction in the $X^4\Delta_{7/2}$ ($v=0$) state was also performed using an effective Hamiltonian approach. For a Hund's case ($a_{\beta J}$) basis set, the diagonal and nondiagonal (in J) matrix elements of the hyperfine parameters a , b_F , and c have the same J depen-

TABLE II. Values determined for the permanent electric dipole moment of FeH (in Debye).

State	Expt. ^a	Theory
$F^4\Delta$	1.29(3)	2.43, ^b 0.2 ^c
$X^4\Delta$	2.63(3)	2.9±0.2, ^d 2.59, ^b 2.0, ^c 3.77 ^e

^aThis work; standard deviation of fit=16.4 MHz; correlation coefficient =0.90.

^bCASSCF-MRCPA(4); Ref. 20.

^cCASSCF/MRCl, Ref. 21.

^dCASSCF/CI-natural orbital iteration; Ref. 16.

^ePseudopotential; Ref. 17.

dence. In order to obtain eigenvalues and eigenvectors, the choice of operator is arbitrary. The splittings within the $J=3.5$ and 4.5 rotational levels of the $X^4\Delta_{7/2}$ ($v=0$) state¹⁵ were modeled using only the Fermi-contact operator,²⁸

$$H^F = b_F \hat{I} \cdot \hat{S}, \quad (2)$$

with $b_F=0.001\,32\text{ cm}^{-1}$. As outlined in Ref. 15, it is not possible to determine the sign of any hyperfine parameters from LMR data. The assignment in this work of a positive value for b_F , and consequentially the energy ordering of the levels, is implied from the least-squares fits of the Stark data. Fits using a model with b_F taken as negative produced a considerably higher standard deviation.

The matrix representations of H^{rot} , H^{LD} , and H^F were co-added and numerically diagonalized to produce eigenvectors and eigenvalues. A similar process was used to produce eigenvectors and eigenvalues for the $F^4\Delta_{7/2}$ ($v=1$) state. In this case, b_F was constrained to zero, the matrix elements for H^{rot} taken as the familiar B equals $J(J+1)$, with $B=5.692\,83\text{ cm}^{-1}$,² and Eq. (1) used to generate H^{LD} .

B. Stark predictions and intensities

The interaction of the molecule with the static electric field was modeled using the conventional Stark Hamiltonian,

$$H^{\text{Stark}} = -\boldsymbol{\mu} \cdot \mathbf{E}, \quad (3)$$

where \mathbf{E} is the external electric field, and $\boldsymbol{\mu}$ is the electric-dipole moment operator of the molecule in question. The matrix representation of H^{Stark} is diagonal in the projection quantum number M_F , but is strictly of infinite dimension. The Stark effect in the required $J=3.5$ levels of the $X^4\Delta_{7/2}$ ($v=0$) level was modeled to the accuracy of the measurements (about 5 MHz) by truncating the representation to include only the eight case (a_{BJ}), nonparity basis functions used to model the $F=3$ and 4 field-free levels. Even though the excited state magnetic hyperfine interactions were too small to resolve, nuclear spin was included in the representation of the $F^4\Delta_{7/2}$ ($v=1$) level to facilitate the intensity predictions. The expressions for the matrix elements of H^{Stark} were taken from the literature.²⁸ Combinations of the calculated energies were compared with the 364 observed shifts in a nonlinear least-squares fitting procedure that optimized the values of $|\mu|$ for the $F^4\Delta_{7/2}$ ($v=1$) and $X^4\Delta_{7/2}$ ($v=0$) states. The optimized values are 2.63(3) and 1.29(3) D for the $X^4\Delta$ ($v=0$) and $F^4\Delta$ ($v=1$) states, respectively, with a correlation coefficient of 0.90 (Table II). The quoted uncertainties rep-

resent a 90% confidence limit stemming from the statistical error. The estimated systematic error of 2% is slightly larger. The standard deviation of the fit was 16.4 MHz, which is commensurate with the measurement uncertainty of the spectral shifts.

The quantum number assignment of the spectra was greatly assisted by modeling the intensities. The transition moments were calculated using

$$\text{TM} = [ev(F^4\Delta_{7/2})] \cdot [\text{TMat}] \cdot [ev(X^4\Delta_{7/2})], \quad (4)$$

where $[\text{TMat}]$ is the transition-dipole moment matrix, $[ev(F^4\Delta_{7/2})]$ is the row vector of eigenvector coefficients for the $F^4\Delta_{7/2}$ ($v=1$) state, and $[ev(X^4\Delta_{7/2})]$ is the column vector of eigenvector coefficients for the $X^4\Delta_{7/2}$ ($v=0$) state. In the field-free case, a 4×4 transition moment matrix was constructed using the four $|\Omega|=3.5$ and Hund's case (a_{BJ}) basis functions for the $X^4\Delta_{7/2}$ ($v=0$) and $F^4\Delta_{7/2}$ ($v=1$) states. In the predictions of the Stark spectra a 8×12 transition moment matrix was constructed using the eight Hund's case (a_{BJ}) basis functions for $F=3$ and 4 levels of the $X^4\Delta_{7/2}$ ($v=0$) state and the twelve Hund's case (a_{BJ}) basis functions for $F=3, 4$, and 5 levels for the $F^4\Delta_{7/2}$ ($v=1$) state. The transition moment was squared, multiplied by a Boltzmann factor for a rotational temperature of 10 K, and used in conjunction with a Lorentzian linewidth of 20 MHz full width at half maximum to predict each spectral feature. The predicted spectra were obtained by co-adding the individual spectral features.

V. DISCUSSION

The permanent electric dipole moments in both the $v=1$ level of the $F^4\Delta_{7/2}$ state [1.29(3) D] and the $v=0$ level of the $X^4\Delta_{7/2}$ state [2.63(3) D] have been accurately determined by a judicious choice of transitions and multiple field strength measurements. Only the magnitude of the permanent electric dipole moment, $|\mu|$, can be determined in a Stark experiment, but it is reasonable to expect that the charge distribution is $\text{Fe}^{+\delta}\text{H}^{-\delta}$. The trend in the dipole moments, with the $\mu(F^4\Delta_{7/2})$ being less than $\mu(X^4\Delta_{7/2})$, indicates that the $\text{Fe}(3d^64s^2)+\text{H}(1s^1)$ bonding contribution is more important in the description of the $F^4\Delta_{7/2}$ state than the $X^4\Delta_{7/2}$ state. The accompanying singly occupied, nonbonding $4s/4p$ hybrid orbital in this bonding scheme points away from the Fe–H bond, thus reducing the dipole moment. A better representation of the difference in charge distribution between the $F^4\Delta_{7/2}$ ($v=1$) and $X^4\Delta_{7/2}$ ($v=0$) states is garnered by comparing the experimental reduced dipole moments ($\equiv \mu/r_c$) which are $1.65\text{ D}/\text{\AA}$ [$X^4\Delta_{7/2}(v=0)$] and $0.742\text{ D}/\text{\AA}$ [$F^4\Delta_{7/2}(v=1)$].

The SCF and CI(SD) calculation using a pseudopotential to represent the Ne-like core predicts 3.77 D for $\mu(X^4\Delta)$ (Ref. 17) and is in poor agreement. Evidently the bias towards the single $a^5F(3d^74s^1)$ configuration of the SCF approach, which predicts a large dipole moment, cannot be overcome in this limited electron correlation treatment. The 2.9 ± 0.2 D prediction obtained from a CASSCF/CI calculation,¹⁶ which used the computationally intensive natural orbital iteration scheme, is in much better agreement be-

ing approximately 12% larger than the determined value. No prediction for $\mu(F^4\Delta)$ was given in Ref. 16. The CASSCF-MRCPA(4) prediction²⁰ for the $X^4\Delta$ state ($=2.59$ D) is in excellent agreement with the observation, but the predicted value for the $F^4\Delta$ state ($=2.43$ D) by the same approach is in very poor agreement. This prediction indicated that the primary configuration for the $X^4\Delta$ state does not have the $4s/4p$ hybrid orbital populated, which is consistent with the observed larger dipole moment. The Brookhaven calculation,²¹ which used a similar CASSCF approach for generating the configuration state functions but employed a multireference single and double excitation configuration interaction (MRSDCI) approach for differential electron correlation, more accurately predicts the reduction of the dipole moment upon excitation. In addition the predicted value for the $X^4\Delta$ state ($=2.0$ D) (Ref. 21) is in good agreement with observation.

The Λ -doubling splitting is a sensitive measure of rotation and spin-orbit induced mixing. The Λ doubling of the lowest rotational levels ($J \leq 8.5$) of the $F^4\Delta_{7/2}$ ($v=1$) state exhibits a general J dependence expected for a homogeneously perturbed state of $^4\Delta$ symmetry²⁷ but with a local perturbation at $J=7.5$. A fit of the observed Λ -doubling intervals in the lowest rotational levels ($J \leq 7.5$) of the $X^4\Delta_{7/2}$ ($v=0$) state given in Ref. 15 to Eq. (1) gives values for δ and δ_D of $2.892(77) \times 10^{-7}$ and $-2.33(13) \times 10^{-9} \text{ cm}^{-1}$, respectively, and no evidence of strong local perturbations. These values are similar to those determined for the $F^4\Delta_{7/2}$ state [$1.534(50) \times 10^{-8}$ and $-1.027(63) \times 10^{-10} \text{ cm}^{-1}$] as expected given that both states are part of the same group of ten interacting low-lying electronic states produced by coupling the H $1s$ electron to the $3d^7 4s^1$ and $3d^6 4s^2$ electrons of Fe. The proton magnetic hyperfine interaction is considerably smaller in the $F^4\Delta_{7/2}$ ($v=1$) state than the $X^4\Delta_{7/2}$ ($v=0$) state indicating that the unpaired electrons are more Fe-centered in the excited state. A prediction of the proton hyperfine interaction for FeH in both the $X^4\Delta$ and $F^4\Delta$ states would be illuminating.

ACKNOWLEDGMENTS

This research has been supported in part by National Science Foundation-Experimental Physical Chemistry (Grant No. CHE 0317130). One of the authors (J.J.H.) thanks the

Leverhulme Trust for financial support and Christ Church College, Oxford for a nonstipendiary fellowship.

- ¹J. G. Phillips, S. Davis, B. Lindgren, and W. J. Balfour, *Astrophys. J., Suppl. Ser.* **65**, 721 (1987).
- ²M. Dulick, C. W. Bauschlicher, Jr., A. Burrows, C. M. Sharp, R. S. Ram, and P. Bernath, *Astrophys. J.* **594**, 651 (2003).
- ³W. Balfour, J. M. Brown, and L. Wallace, *J. Chem. Phys.* **121**, 7735 (2004).
- ⁴R. T. Carter, T. C. Steimle, and J. M. Brown, *J. Chem. Phys.* **99**, 3166 (1993).
- ⁵R. T. Carter and J. M. Brown, *J. Chem. Phys.* **101**, 2699 (1994).
- ⁶D. M. Goodridge, R. T. Carter, T. C. Steimle, and J. M. Brown, *J. Chem. Phys.* **106**, 4823 (1997).
- ⁷D. M. Goodridge, D. F. Hullah, and J. M. Brown, *J. Chem. Phys.* **108**, 428 (1998).
- ⁸D. F. Hullah, C. Wilson, R. F. Barrow, and J. M. Brown, *J. Mol. Spectrosc.* **192**, 191 (1998).
- ⁹D. F. Hullah, R. F. Barrow, and J. M. Brown, *Mol. Phys.* **97**, 93 (1998).
- ¹⁰C. Wilson and J. M. Brown, *J. Mol. Spectrosc.* **197**, 188 (1999).
- ¹¹C. Wilson, H. M. Cook, and J. M. Brown, *J. Chem. Phys.* **115**, 5943 (1998).
- ¹²C. Wilson and J. M. Brown, *J. Mol. Spectrosc.* **209**, 192 (2001).
- ¹³S. P. Beaton, K. M. Evenson, T. Nelis, and J. M. Brown, *J. Chem. Phys.* **89**, 4446 (1988).
- ¹⁴J. P. Towle, J. M. Brown, K. Lipus, E. Bachem, and W. Urban, *Mol. Phys.* **79**, 835 (1993).
- ¹⁵J. M. Brown, H. Körsgen, S. P. Beaton, and K. M. Evenson, *J. Chem. Phys.* (to be published).
- ¹⁶D. P. Chong, S. R. Langhoff, C. W. Bauschlicher, Jr., S. P. Walch, and H. Partridge, *J. Chem. Phys.* **85**, 2850 (1986).
- ¹⁷M. Dolg, U. Wedig, H. Stoll, and H. Preuss, *J. Chem. Phys.* **86**, 2123 (1987).
- ¹⁸S. R. Langhoff and C. W. Bauschlicher, Jr., *J. Mol. Spectrosc.* **141**, 243 (1990).
- ¹⁹M. Sodupe, J. M. Lluch, A. Oliva, F. Illas, and J. Rubio, *J. Chem. Phys.* **92**, 2478 (1990).
- ²⁰K. Tanaka, M. Sekiya, and M. Yoshimine, *J. Chem. Phys.* **115**, 4558 (2001).
- ²¹Z. Wang, T. J. Sears, and J. T. Muckerman (to be published).
- ²²T. C. Steimle, *Int. Rev. Phys. Chem.* **19**, 455 (2000).
- ²³S. Gerstenkorn and P. Luc, *Atlas du spectre d'absorption de la molécule de l'iode* (Editions du C.N.R.S., Paris, 1978); *Rev. Phys. Appl.* **14**, 791 (1979).
- ²⁴S. Gerstenkorn, P. Luc, and R. Vetter, *Rev. Phys. Appl.* **16**, 529 (1981).
- ²⁵T. C. Steimle, J. Gengler, and J. Chen, *Can. J. Chem.* **82**, 779 (2004).
- ²⁶See EPAPS Document No. E-JCPSA6-124-004617 for two pages of observed and calculated Stark shifts. This document can be reached via a direct link in the online article's HTML reference section or via the EPAPS homepage (<http://www.aip.org/pubservs/epaps.html>).
- ²⁷J. M. Brown, A. S.-C. Cheung, and A. J. Merer, *J. Mol. Spectrosc.* **124**, 464 (1987).
- ²⁸J. M. Brown and A. Carrington, *Rotational Spectroscopy of Diatomic Molecules* (Cambridge University Press, Cambridge, 2003).